

Endogenous oxytocin release in periaqueductal gray eases inflammatory pain through long term suppression of pain perception neurons in the spinal cord

M. IWASAKI^{1,2}, A. CHARLET²

¹ The Danish Res. Inst. of Translational Neurosci. Building 1171, 128, Aarhus Univ., Aarhus C, Denmark; ² Inst. of Cell. and Integrative Neurosciences, French Natl. Ctr. for Scientific Res., Strasbourg, France

*corresponding author; mai@biomed.au.dk

Abstract

Research has shown that oxytocin (OT) injection to periaqueductal gray (PAG) eases pain. We hypothesized that OT in PAG may eventually suppress the activity of pain perception neurons inside the spinal cord (SC), then block further aversion signals to the brain. Here, we confirmed that PAG receives OT-ergic axons from the paraventricular nucleus in rats. In PAG, optogenetically triggered axonal OT release evoked excitation in some neurons, and inhibition in others. Of these OT-excited neurons, active neurons alternated between one and the other as time passed, but the number of active neurons at each moment was continuously maintained at the same level at least for 300 s after laser beam stimulation. Further, OT release in PAG reduced pain-induced activity of SC neurons, whose effect reached maximum levels at approximately 220 s after the laser beam stimulation. Interestingly, in rats presented with pain but where OT release was not evoked, a similar time course of SC activity reduction was observed, but the magnitude of reduction was minor. Lastly, OT release in PAG raised the threshold of mechanical pain but not heat pain in inflammation model animals.

Introduction

During World War II, severely wounded soldiers in the US army reported feeling only moderate pain [1], which suggests that our bodies have a natural pain-killing system. Later, it was found that peripheral pain can be eased by a top-down pain modulation system, consisting of periaqueductal gray (PAG) in the midbrain, paraventricular nucleus (RVM) in the medulla, and the dorsal horn of the spinal cord [2]. Oxytocin (OT) in PAG has been implicated in this descending analgesic system, in a context of “pain kills pain” type of negative feedback [3]. OT-ergic neurons in paraventricular nucleus (PVN) project to periaqueductal gray [4], and the concentration of OT in PAG increases in response to pain input [5]. With this in mind, pain input may induce firing of OT neurons in PVN, hence releasing OT locally in PAG. In PAG, administration of OT increased firing of some neurons via OT receptors [6]. One study reported that, when OT was administered to PAG, rats became more resistant to pain caused by electric shock [5]. These studies allow us to infer that OT achieves analgesia through facilitation of neural firing in PAG. However, the downstream targets of PAG are still unclear. However, it has been reported that electrical stimulation of PAG inhibited the firing of neurons in the dorsal horn of spinal cord, although the

study did not investigate OT [7], which induced analgesia [8]. Therefore, we hypothesized that OT in PAG eventually inhibits pain perception neurons in the spinal cord and thus creates an analgesic effect in animals. Specifically, we aimed to i) histologically confirm the endogenous source of OT to the PAG, ii) observe the firing dynamics of neurons in periaqueductal gray in response to endogenous OT release in periaqueductal gray, iii) examine whether OT release in periaqueductal gray induces the suppression of pain perception neurons in the spinal cord, iv) and test whether inflammatory pain can be eased by endogenous OT release in PAG.

Results

OT neurons of the PVN give rise to long-range axonal projections terminating in the Periaqueductal Grey

To examine OT axonal projections from PVN (PVN-OT) to PAG, we used recombinant adeno-associated virus (rAAV), which expresses Venus fluorescent protein under the control of an OT promoter (Figure 1A) [9]. Following rAAV injections in PVN (Figure 1B), we observed that OT neurons of the PVN (Figure 1C) send fibers to the ventro-lateral PAG (vlPAG) (Figure 1D).

Blue light in PAG induced excitation or inhibition of PAG neurons at multiple time courses

We aimed for a functional characterization of PVN-OT projections to PAG. We expressed the blue light (BL)-sensitive ChR2 protein [10] fused to mCherry (Figure 2A) in PVN-OT neurons (Knobloch et al., 2012). While neural spikes in PAG were recorded in anesthetized rats, BL (20 s at 30 Hz with 10 ms pulses) was flashed in PAG to stimulate PVN-OT axons (Figure 2B and 2C). Of 82 recorded neurons, 21 neurons increased their firing rate (mean \pm SEM; from 1.05 ± 0.39 to 17.65 ± 6.45 Hz) (Figure 2D1 and 2D2), whereas two neurons whose spontaneous activity prior to BL onset was high, decreased their firing rate within 300 s after BL flash (one cell from 25.83 to 6.95 Hz, another from 40.20 to 0.19 Hz), and 59 neurons were not reactive to the BL flash (Figure 2F). Based on the normalized activity (Figure 2E), we found that the mean activity of the excited neural population remained elevated for at least 300 s from the initiation of the BL flash to the end point of recording (Figure 2G). Interestingly, the time course of spike increase was diverse; latency (1st quantile, median, 3rd quantile) (s) for onset (1, 4, 40.25), for peak moment (116.25, 155, 280.25), and for offset (147.75, 296, 300) (Figure 2H). On the other hand, total number of active neurons was maintained throughout 300 s after BL flash (Figure 2I). This data, therefore, suggests that the PVN-OT-evoked populational excitation in PAG was made with the facilitation of multiple neurons whose active timing varied from cell to cell.

PVN-OT neurons projecting to PAG neurons suppress nociceptive neurons in deep layers of the Spinal Cord, which controls Central Nociceptive Processing

To test whether the PVN-OT axons in PAG eventually act on nociceptive inputs, we stimulated PVN-OT axons in PAG of ChR2-expressing rats by shining BL (PAG-BL), while we recorded neuronal responses from the spinal cord (SC) to electrical stimulation of the hindpaw

receptive fields (Figure 2A1 and 2A2). Peripheral sensory information converges from primary afferent fibers: fast-conducting (A-type) and slow-conducting (C-type) fibers. Primary inputs become integrated with wide-dynamic-range (WDR) neurons in deep laminae of SC. Following repetitive electric stimulation to the hindpaw receptive field, a short-term potentiation (wind-up; WU) occurs on the synapse made by C-type fibers on WDR neurons, which is typically enhanced during pain perception in animals with inflammation [11]. Therefore, we utilized WU as an index of ongoing nociception processing, showing how sensitive or numb the body is to the pain-causing stimulus at a given moment. First, we tested to see if PAG-BL had an effect on WDR discharge from specific primary afferent fibers ($A\beta$ -fibers in 0-20 ms, $A\delta$ -fibers in 20-90 ms, C-fibers in 90-300 ms and C fiber post discharge in 300 to 800 ms after each single electric shock, added at 1 Hz), and which kind of time course the PAG-BL effect had. For this purpose, we averaged raster plots two dimensionally, across neurons within each group of rats, and further normalized it so that the plateau phase of WU was 100 percent activity. We found that PVN-OT excitation by PAG-BL in ChR2 rats had some inhibitory effect on WDR discharge related to C-fibers (WU), whose spikes range between 90-800 ms post- electric shock (Figure 3B2, left panel), compared to WT animals (Figure 3B1, left panel). This trend was maintained during the second recording, which was performed 530 to 590 s after the BL turned off (Figure 3B2 right panel). The inhibitory effect was partly diminished when the OTR antagonist, dOVT, was injected into PAG prior to stimulation (Figure 3B3).

Next, we focused on the time course of the PAG-BL's inhibitory effect on WU (Figure 3C). In wild type rats, once WU reached the maximum plateau activity level around 30 s after the first electric shock, the activity remained high but at the same time, gradually dropped until it reached the lowest activity level approximately 240 s after the first WU. When PVN-OT was stimulated by PAG-BL in ChR2 rats, the maximum WU reduction became significantly larger ($p=0.0074$, from 30.12 ± 8.60 to 61.28 ± 5.37 % reduction compared to the plateau of WU) (Figure 3D, blue). When dOVT was administered to PAG, the effect of PAG-BL was significantly impaired ($p=0.0313$, 36.27 ± 4.80 % reduction) (Figure 3D, red). We defined the period of maximum WU reduction as 140 to 180 s after PAG-BL started, because after this period, in ChR2 rats with dOVT, the injected dOVT lost its OT-blocking effect, possibly due to diffusion. While the magnitude of WU reduction was significantly larger in ChR2 animals than WT animals, there was no difference in "inflection" timing of WU dynamics (1st quantile, median, 3rd quantile) (s); Latency (s) to reach the maximum WU was not significantly different between WT= (26.00, 31.50, 46.00) and ChR2= (26.25, 35.00, 55.75). Latency to reach the half reduction of WU was not significantly different between WT= (75.50, 96.50, 163.00) and ChR2= (64.25, 83.00, 125.75). Latency to reach the max reduction of WU was not significantly different between WT= (183.00, 209.00, 263.00), ChR2= (198.50, 250, 269.75) (Figure 3E). In summary, excitation of PVN-OT axons in PAG inhibited nociception related activity (C-fiber mediated discharge on WDR neurons) in the deep layers of SC. Because the inhibition was impaired by dOVT injected to PAG, this process is likely mediated by OT release from PVN-OT axon in PAG.

PAG BL raised the threshold of mechanical but not heat pain in inflammation model

In rats expressing ChR2, we measured the effects of PAG-BL excitation of PVN-OT axons in the processing of inflammatory pain. The symptoms of a peripheral painful inflammatory sensitization was triggered by a unilateral intra-plantar injection of complete Freund adjuvant (CFA) (Figure 4A). PAG-BL stimulation alleviated the CFA-mediated hyperalgesia by raising the threshold of response to the mechanical pain on day one (mean \pm SEM (g)) from 68.77 \pm 9.39 (base) to 124.89 \pm 12.76 (BL) ($p < 0.0001$), which was statistically significant. On day two, when the blood brain barrier (BBB)-permeable OTR antagonist, L-368,899 was intraperitoneally injected, the effect of PAG-BL was fully blocked from 62.75 \pm 5.31 (base) to 71.99 \pm 5.14 (BL) ($p = 0.83$). Furthermore, on day three, when L-368,899 had been washed out, the effect of PAG-BL was fully recovered from 92.95 \pm 8.89 (base) to 179.40 \pm 19.13 (BL) ($p < 0.0001$) (Figure 4B, red). In contrast, PAG-BL failed to raise the threshold of thermal hot sensitivity (Figures 4C, red). We observed that PAG-BL failed to modify mechanical and thermal hot sensitivity in the absence of any peripheral sensitization, in the contralateral paw (Figures 4B, 4C, gray). These findings provide evidence that PVN-OT axons in PAG promotes analgesia in a pathological condition of inflammatory pain, which is supported by our in vivo electrophysiological data.

Discussion

The analgesic effect of OT in PAG toward pain perception neurons has not been adequately examined to date. Therefore, we first confirmed by virus based anatomical observation that OT neurons in PVN do project axons to PAG, which was previously found by another anterograde tracer study [4]. Next, because OT injection made rats less sensitive to aversive electric shock [5], we confirmed that endogenous OT release in PAG can decrease mechanical sensitivity in inflammatory pain model animals. However, thermal sensitivity was not modified by OT. This is likely because there are independent analgesic systems for each mechanical and thermal pain. For example, previous work has suggested that the relief of mechanical pain requires norepinephrine release in dorsolateral PAG [12], whereas the relief of thermal pain requires serotonin release in ventrolateral PAG [13].

Further, we found that nociceptive transmission from C-type primary afferents to WDR neurons in spinal cord was efficiently repressed by endogenous OT release in PAG. PAG projects to rostral ventral medulla (RVM) [14] and RVM sends axons to the spinal cord (SC) [15]. Electric stimulation of PAG inhibits the firing of dorsal horn neurons in SC [7], and generates analgesia [8]. Because this analgesic effect was interrupted by lesions of RVM [16], RVM is considered an essential link between PAG and SC. Viral tracing work has shown that analgesic projections from PAG to RVM is glutamatergic [17]. Pharmacological work has suggested that PAG to RVM glutamatergic projection neurons are typically inhibited by local GABAergic neurons, which are tonically active, and that the glutamatergic projection neurons get excited when GABAergic

inhibition is removed [18]. In addition, an *in vitro* electrophysiology study reported that administration of OT “excited” spontaneous activity of PAG neurons [6]. In the current study, optogenetic OT release in PAG triggered not only excitation of some neurons whose spontaneous spike rates were low, but also caused inhibition of other neurons whose spontaneous spike rates were high. An important future investigation would be to determine whether the OT-excited neuronal population in our study is from the same population of glutamatergic neurons found in the Grajales-Reyes and colleagues’ study above and similarly, if the OT-inhibited neurons in our study correspond to the local GABAergic neurons found in the Lau and Vaughan study above.

In our study, the activity of each OT-excited neuron in PAG increased at various times, from approximately (1st to 3rd quantile) from 1 to 40 s after BL stimulation. The neurons’ offset timings were also diverse, approximately (1st to 3rd quantile) from 150 s to more than 300 s. The reason for such variation in offset time is likely because OT receptors are G-protein coupled metabotropic receptors, which typically produce “slow” post synaptic currents for up to the minute order, while ionotropic receptors such as glutamatergic or GABAergic receptor produces “fast” post synaptic current less than 100 ms [19]. On the other hand, the reason for high onset variation is likely because OT is a neurotransmitter that has extra-synaptic volume transmission, whose signal targets are diffuse multiple neurons expressing OT receptors. In fact, it is known that OT neurons release not only OT but also classical neurotransmitters such as glutamate or GABA from their synapses [20]. However, it has been shown that OT-excited neural activity in PAG was not abolished by synaptic blockade [6]. Generally, volume transmission occurs for seconds to minutes while one-on-one synaptic transmission is in the milliseconds range. Furthermore, it has been reported that volume transmission of neuropeptides, such as OT, reach their target further than 1 mm from the peptide-releasing source [21]. Although it is reported that OT fibers were located closely to OTR expressing neurons in vIPAG [4], OT can travel further than the closest OTR expressing neurons. In our study, for example, it is possible that if some distant OT fibers were stimulated by BL penetrating through the brain tissue, the released OT may only arrive the OTR expressing neuron after a long time-delay. The range of relative distance between OT axons and OTR expressing neurons may explain the variance in onset of BL-triggered activity in PAG. Therefore, “One-shot” of OT release could be relayed across multiple OTR expressing neurons, resulted in long-lasting excitation as the sum of different active timings.

When we try to interpret the OT-PAG analgesic system, an intriguing possibility is that OT achieves an analgesic effect via mu opioid receptors, which is also a G-protein coupled metabotropic receptor whose post synaptic current can last up to minutes. A recent study found that, although OT alone does not directly bind to the opioid-binding site of mu opioid receptor, OT strongly enhances the signaling of mu opioid receptor [22]. In addition to those studies using electric stimulation of PAG, mu opioid receptor agonist injection to PAG has also confirmed the descending analgesic pathway; PAG, RVM, and SC as follows. In RVM, there are two types of neurons. One is called “on-cell”, which becomes active against aversive input, and another is

called “off-cell”, which becomes silent in response to pain perception [23] and which directly projects to nociception neurons in the spinal cord [2]. Mu opioid receptor agonist administration into PAG leads to RVM “off-cells” to continuously fire, inducing analgesia. Selective blockade of “off-cell” prevented this anti-nociception [23]. Therefore, the opiate-PAG analgesic system is likely be mediated via RVM off-cells. Judging by the fact that, in the current study, OT-excited neural activity was long lasting in PAG, the OT-PAG analgesic system may also be mediated by continuous firing of RVM off-cells. Generally, activation of mu opioid receptors expressing at the terminals of GABAergic neurons, reduces release of GABA [24]. The aforementioned GABAergic disinhibition of PAG to RVM excitatory projection neurons, which is required for analgesia, could be triggered in this way by endogenous opioids: enkephalins, dynorphins, or beta-endorphins whose axon are found in PAG [25]. Then, OT release in PAG may enhance the opiate-PAG analgesic system.

In spinal cord WDR neurons, WU inhibition started during BL flash, and was maximally inhibited 250 s (median) after BL flash initiated. Further, this inhibition was still observed even 590 s after BL was turned off. As mentioned above, considering that OT was released only for 20 s, an “OT-excited” neural population in PAG stayed active much longer, for at least 300 s after the BL flash was initiated. Therefore, long-lasting WU inhibition in the spinal cord could be continually driven by ongoing excitation of “OT-excited” neural population in PAG.

While the magnitude of WU reduction was significantly larger in ChR2 animals than WT animals, there was no difference in “inflection” timing of WU dynamics. This means that, even at the natural condition where OT was not artificially released, WU activity naturally decreased following a similar reduction time course to that observed in ChR2 animals. One possible interpretation is that the natural WU reduction could be caused by OT, which was naturally released in PAG without optogenetic stimulation. In fact, when a nociceptive stimulus was added to rats’ hindpaw, the concentration of OT in PAG increases in response to nociceptive input [5]. Therefore, this implies that OT release in PAG may be a part of negative feedback system, which was suggested in a previous study; nociceptive input numbs pain perception [3]. Another interpretation is that the natural decrease of WU may be triggered by another analgesic system, such as opiate-PAG analgesic system, and OT release in PAG may enhance the system.

Materials and Methods

Animals

Anatomical, electrophysiological, optogenetic, and behavioral studies were performed with adult female Wistar rats. Rats were housed under standard conditions with food and water available ad libitum, and maintained on a 12-hour light/dark cycle. All experiments were conducted under licenses and in accordance with EU regulations.

Viruses

Recombinant Adeno-associated virus (serotype 1/2) carrying conserved region of OT promoters and genes of interest (Venus, or Channelrhodopsin2-mCherry) in direct orientations were cloned and produced as reported previously [9].

Neuroanatomy

rAAVs expressing Venus were injected into the PVN to follow their axonal projections to the PAG. The coordination of PVN was chosen using the rat brain atlas [26](ML: +/-0.3 mm; AP: -1.4 mm; DV: -8.8 mm). After transcardial perfusion with 4% paraformaldehyde (PFA), brain sections (50 μ m) were collected by vibratome slicing and immunohistochemistry was performed, first with the following primary antibodies: anti-VGluT2 (1:2000; rabbit; SySy), or anti-NeuN (1:1000; rabbit; Abcam). As secondary antibodies, Venus signal was enhanced by Alexa488-conjugated IgGs. Other primary antibodies were visualized using CY3-conjugated or CY5-conjugated antibodies (1:500; Jackson Immuno-Research Laboratories). All images were acquired on a confocal Leica TCS microscope; digitized images were processed with Fiji and analyzed using Adobe Photoshop. For the visualization of OT-ergic axonal projections within the PAG, we analyzed brain sections ranging from Bregma -6.0mm to -8.4mm.

In vivo extracellular recording of OT axons in PAG

300 nl of AAVs, carrying ChR2-mCherry driven by the OT promoter was unilaterally injected into the PVN (ML: +/-0.3 mm; AP: -1.4 mm; DV: -7.8 mm). Four to eight weeks after injection of virus, rats were anaesthetized with 4% isoflurane and was placed in a stereotaxic frame. During the procedure, the isoflurane level was reduced to 2%. A silicone tetrode coupled with an optical fiber (neuronexus, USA) was inserted into the PAG to allow for stimulation of the ChR2 expressing axon of PVN-OT neurons projecting to PAG and record their activity under anesthesia Optical stimulation was provided using a blue laser (λ 473 nm, output of 100 mW/mm², Dream Lasers, Shanghai, China) for 20 s at 1 Hz, with 5 ms pulse. Extracellular neuronal activity was recorded using a silicone tetrode coupled with an optic fiber (Q1x1-tet-10mm-121-OAQ4LP; neuronexus, USA). Data were acquired on a MC Rack recording hardware (Multi Channel Systems), and spike was sorted by Wave Clus [27], and analyzed by self-written MATLAB (MathWorks) scripts, using MLIB toolbox for analyzing spike data [28].

In vivo extracellular recording of Dorsal Horn Spinal Neurons

Adult Wistar rats were anesthetized with 4% isoflurane and a laminectomy was performed to expose the L4-L5 SC segments. During the procedure, the isoflurane level was reduced to 2%. Rats were then placed in a stereotaxic frame with the L4-L5 region being held by two clamps placed on the apophysis of the rostral and caudal intact vertebrae. The dura matter was then removed. To record wide-dynamic-range neurons (WDR), a silicone tetrode (Q1x1-tet-5mm-121-Q4; neuronexus, USA) was lowered into the medial part of the dorsal horn of the SC, at a depth of around 500 -1100 μ m from the dorsal surface (see Figure3 A2 for localization of recorded WDR).

We recorded WDR neurons of lamina V, receiving both non-noxious and noxious information from the ipsilateral hind paw.

We measured the action potentials of WDR neurons induced by stimulation of the hindpaw. When the peripheral tactile receptive fields are stimulated repeatedly at specific intensities and frequencies (1 ms pulse duration, frequency 1 Hz, intensity corresponding to 3 times the C-fiber threshold), an increase firing of WDR neurons is observed, which is named Wind-up (WU) [29, 30]. As WU is dependent on C-fiber activation, it can be used as a tool to assess nociceptive information in the SC and OT antinociceptive properties. Therefore, we recorded WDR neurons during the following protocol: 40 s of electric shock on the foot to induce WU, 20 s of WU plus blue light flash (10 ms pulses at 30 Hz, ~100 mW/mm²) in the PAG, and 230 s of WU; a total of 290 s recording session. 300 s after the end of the recording session, 60 s of WU was added to check if the WDR neuron's ability to wind up recovered. To confirm that the reduction in WU intensity was OTR related, we injected 600 nl of dOVT 1 μ M (d(CH₂)₅-Tyr(Me)-[Orn⁸]-vasotocine; Bachem, Germany), and repeated the stimulation protocol after 10 min. Hardware and software were the same as above.

Nociceptive Behavioral Tests

For in vivo behavioral experiments, we used a blue laser (λ 473nm, output of 100 mW/mm², DreamLasers, Shanghai, China) coupled with optical fibers (BFL37-200-CUSTOM, EndA=FC/PC, and EndB=Ceramic Ferrule; ThorLabs, USA; final light intensity ~ 100m W/mm², 30 Hz, 10 ms pulses, 20 s duration), which were connected to a chronically implanted optic fiber to target the PAG (CFMC12L10, Thorlabs, USA). Optic fibers were chronically and bilaterally implanted into the PAG under isoflurane anesthesia (4% induction, 2% maintenance) at stereotaxic positions of -6.7 mm AP and 2.0 mm ML from midline with an medio-lateral 20° angle so that ferrules did not bump each other, and then stabilized with dental cement. This was intended to allow specific stimulation of the PAG, as prevalent measurements with blue laser stimulations in rodent brain have shown that the blue light of the laser does not penetrate the tissue further than 500 μ m [31].

Peripheral painful inflammatory sensitization was obtained by a single unilateral intraplantar injection of CFA (Sigma-Aldrich, 100 μ l in the right paw) and its associated mechanical allodynia and thermal allodynia/hyperalgesia was measured 24 h later, 48 h later with non-peptide oxytocin receptor (OTR) antagonist, L-368,899 (1-((7,7-Dimethyl-2(S)-(2(S)-amino-4-(methylsulfonyl)butyramido)bicyclo[2,2,1]heptan-1(S)-yl)methylsulfonyl)-4-(2-methylphenyl)piperazine hydrochloride), (MERCK, Germany), and 72 h later in the washout condition.

Mechanical allodynia was measured using a pair of calibrated forceps (Bioseb, France), with the protocol previously developed in our laboratory to test animal mechanical sensitivity [32]. Briefly, the habituated rat was loosely restrained with a towel masking the eyes in order to limit stress by environmental stimulations. The tips of the forceps were placed at each side of the paw and a graduated force is applied. We used the pressure (grams) that produced paw withdrawal as the nociceptive threshold value. This manipulation was performed three times for each hind

paw and the mean of these values were used for analysis. Thermal allodynia/hyperalgesia was measured by the plantar test (Ugo Basile, Italy) using the Hargreaves method [33]. Exposed to a radiant heat, the latency time of paw withdrawal was measured three times per hind paw and the mean of these values were used for analysis.

Statistical Analysis

A paired-sample t-test was used to compare the average spike rates between the baseline and peak activity of PAG neurons in response to BL stimulation (Fig2.D1). An unpaired-sample nonparametric test (Wilcoxon rank sum test) was used to compare the reduction discharge of SC neurons between the wild type and the ChR2-expressing animals. A paired-sample nonparametric test (Wilcoxon signed rank test) was used to compare the reduction discharge of SC neurons in the ChR2-expressing animals, between “without dOVT” and “with dOVT” condition (Fig.3D). Wilcoxon rank sum tests were used to compare the latencies to reach the maximum, minimum, and the half value between value between the wild type and the ChR2-expressing rats (Fig.3D). Two-way ANOVA followed by Tukey’s multiple comparison post hoc test was used to analyze behavioral data (Fig.4B, C). Differences were considered significant for $p < 0.05$.

Figure legends

Figure 1. Anatomy of OT neurons projecting from PVN to PAG

- (A) Scheme showing the virus construct injected to the PVN, which allows OT neurons to express Venus.
- (B) Scheme showing the injection of viruses in the PVN, and the relative position of the following microscopic images (C,D).
- (C and D) Brains of rats expressing OTp-Venus in the PVN were sectioned and stained against vGLUT2 and NeuN.
- (C) Image shows OT neurons (green) in the posterior part of the PVN (AP: -1.9 mm). Scale bar represent 50 μm .
- (D) Image shows OT fibers (green) terminating in the region surrounding the cerebral aqueduct (i.e. PAG, AP: -6.8 mm). NeuN (neuron; blue), vGlut2 (glutamatergic neuron; red), Scale bar represent 100 μm .

Figure 2. Electrophysiological characteristics of PAG neurons reacting to activation of PVN OT neurons

- (A) Scheme of the viral construct injected into PVN, which allows OT neurons to express ChR2 mCherry.
- (B) Setup of in vivo electrophysiological recordings (gray; electrode) in PAG, together with blue light stimulation (blue; optic fiber) in the PAG. Recorded coordination is shown on coronal drawings (order: anterior to posterior).
- (C) Raster plot of each single PAG neuron ($n=23$) that responded to BL in PAG. 473 nm of BL was added as 10 ms pulse at 30 Hz for 20 s, 100 $\mu\text{W}/\text{mm}^2$.
- (D1) Difference in mean firing rate between the period before blue light flash (-100 to 0 s relative to the start of blue light) and the maximum activity period after blue light flash (highest value among moving means with a time window of 21 s, between 0 to +300 s after the start of blue light).

(D2) Magnified image of panel D1.

(E) Normalized firing rate of panel C. The firing rate of each recording unit was smoothed by convolution of Gaussian distribution, whose width is 10 s and whose standard deviation is 5. The mean firing rate of baseline period (BS_{mean}) was defined as 0% activity, and it was subtracted from the firing rates (FR) of whole period ($FR - BS_{mean}$). Maximum absolute activity ($\max(|FR - BS_{mean}|)$) was found (highest absolute value among moving means of $(FR - BS_{mean})$ with a time window of 21 s). When maximum ($|FR - BS_{mean}|$) was found above BS_{mean} , maximum $(FR - BS_{mean})$ was defined as 100% activity (cell#1~21), whereas when maximum ($|FR - BS_{mean}|$) was found below BS_{mean} , $\min(FR - BS_{mean})$ was defined as -100% activity (cell#22~23).

(F) Recorded units' responsiveness. Out of total 82 units, the spike rates of 21 units increased and 2 units decreased, following blue light flash stimulation.

(G) Mean percent activity (line) \pm SEM (shaded) calculated from panel E.

(H) Onset and peak and offset of BL-induced excitation in PAG. Onset is defined as the first time code when the spike rate reached above the threshold ($BS_{mean} + 4BS_{SD}$); BS_{mean} is the mean firing rate of baseline period, and BS_{SE} is the standard deviation of firing rate during the baseline period. Offset is defined as the last time code when the spike rate decreased below the threshold for more than 20 s continuously, before 300 s post blue light flash.

(I) Number of active cells in each single second. Here, "active" means that the spike rate was above the threshold ($BS_{mean} + 4BS_{SD}$).

Figure 3. Stimulation of PVN-OT axons in PAG modulates responses of WDR neurons

(A1) Setup of in vivo electrophysiological recordings (gray; electrode) of WDR neurons in the rat spinal cord (SC) at the level of lumbar 4 (L4). In the PAG, blue light was shed (blue; optic fiber) to the ChR2 expressing axons which come from PVN OT neurons. We recorded WDR neurons during the following protocol: 40 s of electric shock on the foot to induce wind up (WU), 20 s of electric shock on the foot plus blue light flash into the PAG, and 230 s of electric shock on the foot: a total of 290 s recording session. 300 s after the end of the first recording session, 60 s of electric shock was added on the foot to test whether WDR's ability to wind up recovered.

In order to confirm that the reduction in WU intensity was related to an OT release in the PAG and acting on OTR, we injected 600 nl of 1 μ M dOVT (d(CH₂)₅-Tyr(Me)-[Orn₈]-vasotocine; Bachem, Weil am Rhein, Germany) locally to the PAG.

(A2) Recorded coordination are shown on a coronal drawing of L4, in the layer 5.

(B1-B3) Mean smoothed raster plot of WDR discharge level along the relative timing to each single electric shock on the hind paw (vertical axis) and along the accumulating trials of electric shock (horizontal axis), in wild type animals (**B1, n=8**), ChR2 animals (**B2, n=14**), or ChR2 rats after dOVT injection in PAG (**B3, n=6**). After each single electric shock, A β fiber discharge appears in 0-20 ms, A δ fiber in 20-90 ms, C fiber in 90-300 ms and C fiber post discharge in 300 to 800 ms.

First, the spikes of each recording unit were described as raster plots whose vertical axis shows the time relative to electric shock, and whose horizontal axis counts the number of electric shocks at 1 Hz. Next, those raster plots were smoothed by convolution of Gaussian distribution, whose horizontal width was 100

ms and vertical width was 20 ms and standard deviation of 20.

(C) Mean time course of the spike rate of WDR's C fiber discharge. First, for each recording unit and for single electric shock on the hind paw, total number of C fiber derived spikes (the spikes in the time period between 90 and 800 ms relative to the electric shock) were counted. After smoothing those spike counts with moving average of a window size 21 s, the maximum activity period was chosen. Next, the mean spike rate of the maximum activity period (21 s) was defined as 100 percent activity, and activity of each recording unit was normalized to the percentage unit. Further, the percentage activity were averaged across all the recording units, within each experimental conditions; wild type rats (gray, n=8), ChR2 expressing animals (blue, n=14), or ChR2 expressing rats after dOVT injection in PAG (red, n=6). Shadow shows SEM.

(D) After reaching to the wind up plateau phase, the activity, which dropped to the minimum level was described as the percentage reduction. We defined minimum activity period as 140 - 180 s after the blue light started to flash (shown in the panel C), because after this period, injected dOVT lost its OT-blocking effect possibly due to diffusion. The percentage reduction of ChR2 rats were significantly more than that of WT rats (Wilcoxon rank sum test; $p=0.0074$) and ChR2 rats with dOVT injection (Wilcoxon signed rank test $p=0.0313$). mean \pm SEM (%); WT= 30.12 ± 8.60 , ChR2= 61.28 ± 5.37 , dOVT= 36.27 ± 4.80 . The statistical significance was described as * $p<0.05$, ** $p<0.01$.

(E) Latencies to reach the maximum activity, minimum activity, and its half activity are shown as box plot. Horizontal line lies between the minimum and maximum latency. Colored box shows the range between 1st and 3rd quantile, and median is shown as vertical line. (1st quantile, median, 3rd quantile); Latency (s) to reach the maximum activity WT=(26.00, 31.50, 46.00), ChR2=(26.25, 35.00,55.75); the half activity WT=(75.50, 96.50,163.00), ChR2=(64.25, 83.00, 125.75); and the minimum activity WT=(183.00, 209.00, 263.00), ChR2=(198.50, 250, 269.75). The mean latency is marked as "+"; Mean latency (s) to reach the maximum activity WT=39.88, ChR2=44.40; the half activity WT=121.25, ChR2=95.27; and the minimum activity WT=209.00, ChR2=232.87.

There was no significant difference for each latency between WT and ChR2. Unpaired nonparametric test (Wilcoxon rank sum test) was applied to the latencies to reach the maximum value WT vs ChR2 $p=0.85$, the half value WT vs ChR2 $p=0.32$, the minimum value WT vs ChR2 $p=0.50$

Figure 4. Activation of PVN-OT neurons result in mechanical analgesia in rats subjected to complete adjuvant injection

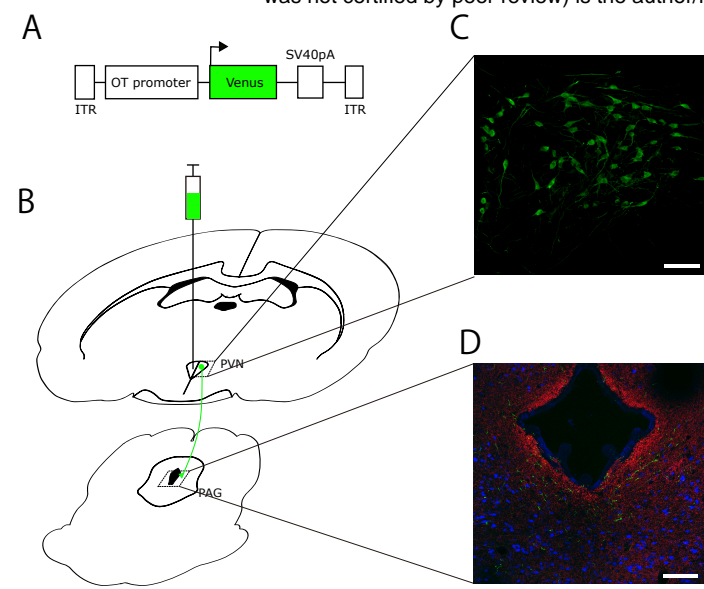
(A) Scheme of the procedure of pain threshold test on inflammatory pain model animals (n=10).

(B) Threshold of mechanical pain was raised by PAG-BL. The effect of PAG-BL was measured at 5 min, 1 h and 3 h after PAG-BL. Blue background represents BL stimulation made of 10 ms pulses at 30 Hz for 20 s. On the inflammation-induced paw (red), the mechanical threshold was assessed on day one. On day two, the threshold was measured but with the intraperitoneal injection of OTR antagonist L-368,899 (1 mg/kg). Furthermore, on day three when the antagonist was already washed out, the threshold was assessed again. The hindpaw of healthy side was used as control (grey). Day1; $p(\text{base vs. BL}) <0.0001$ from 68.77 ± 9.39 to 124.89 ± 12.76 . Day3; $p(\text{base vs BL}) <0.0001$ from 92.95 ± 8.89 to 179.40 ± 19.13 .

(C) Threshold of heat pain was not modulated by PAG-BL. The effect of PAG-BL was measured at 5 min after PAG-BL. All results are expressed as average \pm SEM. Two-way ANOVA was followed by Tukey's multiple comparison post hoc test. The statistical significance in comparison with the base line was described as **** $p < 0.0001$.

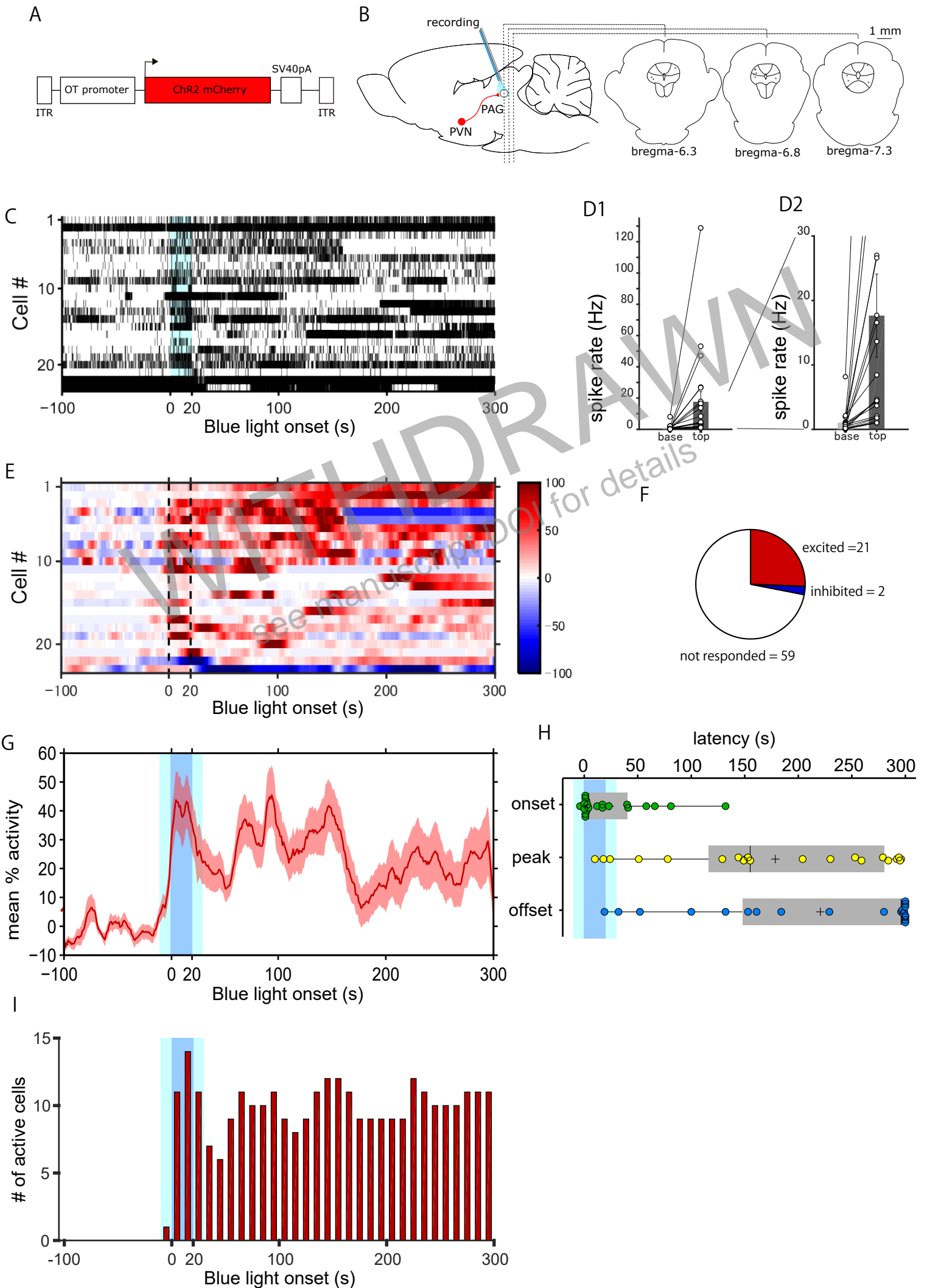
1. Beecher, H.K., *Pain in Men Wounded in Battle*. Ann Surg, 1946. **123**(1): p. 96-105.
2. Fields, H.L., *Pain modulation: expectation, opioid analgesia and virtual pain*. Prog Brain Res, 2000. **122**: p. 245-53.
3. Melzack, R., *Prolonged relief of pain by brief, intense transcutaneous somatic stimulation*. Pain, 1975. **1**(4): p. 357-73.
4. Nasanbuyan, N., et al., *Oxytocin-Oxytocin Receptor Systems Facilitate Social Defeat Posture in Male Mice*. Endocrinology, 2018. **159**(2): p. 763-775.
5. Yang, J., et al., *Oxytocin in the periaqueductal grey regulates nociception in the rat*. Regul Pept, 2011. **169**(1-3): p. 39-42.
6. Ogawa, S., L.M. Kow, and D.W. Pfaff, *Effects of lordosis-relevant neuropeptides on midbrain periaqueductal gray neuronal activity in vitro*. Peptides, 1992, **13**(5): p. 965-75.
7. Liebeskind, J.C., et al., *Analgesia from electrical stimulation of the periaqueductal gray matter in the cat: behavioral observations and inhibitory effects on spinal cord interneurons*. Brain Res, 1973. **50**(2): p. 441-6.
8. Basbaum, A.I., et al., *Reversal of morphine and stimulus-produced analgesia by subtotal spinal cord lesions*. Pain, 1977. **3**(1): p. 43-56.
9. Knobloch, H.S., et al., *Evoked axonal oxytocin release in the central amygdala attenuates fear response*. Neuron, 2012. **73**(3): p. 553-66.
10. Nagel, G., et al., *Channelrhodopsin-2, a directly light-gated cation-selective membrane channel*. Proc Natl Acad Sci U S A, 2003. **100**(24): p. 13940-5.
11. Herrero, J.F., J.M. Laird, and J.A. Lopez-Garcia, *Wind-up of spinal cord neurones and pain sensation: much ado about something?* Prog Neurobiol, 2000. **61**(2): p. 169-203.
12. Kuraishi, Y., *[Neuropeptide-mediated transmission of nociceptive information and its regulation. Novel mechanisms of analgesics]*. Yakugaku Zasshi, 1990. **110**(10): p. 711-26.
13. Kuraishi, Y., et al., *Separate involvement of the spinal noradrenergic and serotonergic systems in morphine analgesia: the differences in mechanical and thermal algesic tests*. Brain Res, 1983. **273**(2): p. 245-52.
14. Mantyh, P.W., *Connections of midbrain periaqueductal gray in the monkey. II. Descending efferent projections*. J Neurophysiol, 1983. **49**(3): p. 582-94.
15. Zorman, G., et al., *Naloxone-reversible analgesia produced by microstimulation in the rat medulla*. Brain Res, 1981. **219**(1): p. 137-48.
16. Prieto, G.J., J.T. Cannon, and J.C. Liebeskind, *N. raphe magnus lesions disrupt stimulation-produced analgesia from ventral but not dorsal midbrain areas in the rat*. Brain Res, 1983. **261**(1): p. 53-7.
17. J. G. GRAJALES-REYES, V.K.S., B. A. COPITS, M. R. BRUCHAS, R. W. GEREAU. *Analysis of the role of glutamatergic and GABAergic ventrolateral periaqueductal gray (vIPAG) neuronal subpopulations*

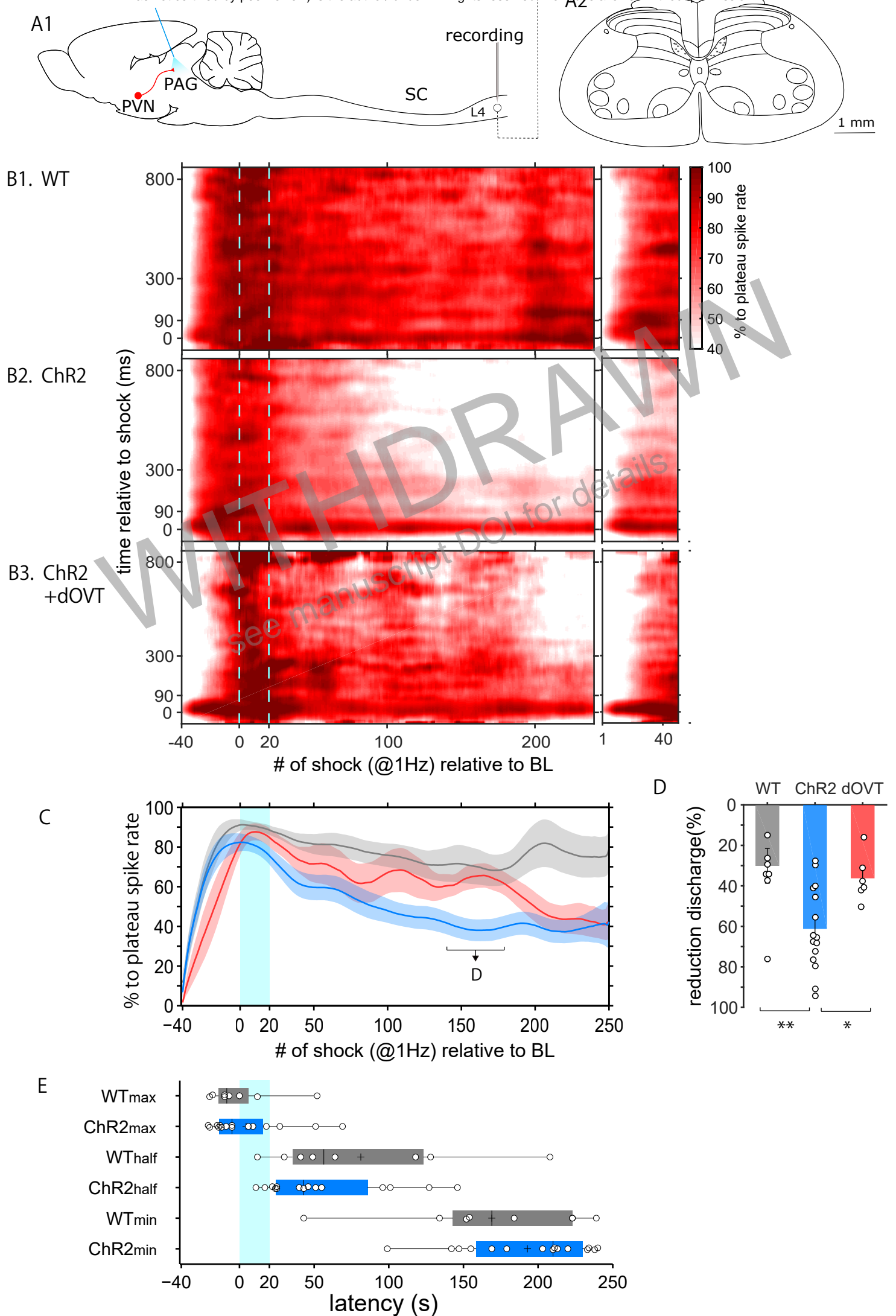
- in a mouse model of persistent inflammatory pain.* in *Society for Neuroscience annual meeting, program # 390.10.* 2018.
18. Lau, B.K. and C.W. Vaughan, *Descending modulation of pain: the GABA disinhibition hypothesis of analgesia.* *Curr Opin Neurobiol*, 2014. **29**: p. 159-64.
 19. Jan, Y.N., L.Y. Jan, and S.W. Kuffler, *A peptide as a possible transmitter in sympathetic ganglia of the frog.* *Proc Natl Acad Sci U S A*, 1979. **76**(3): p. 1501-5.
 20. Hokfelt, T., *Neuropeptides in perspective: the last ten years.* *Neuron*, 1991. **7**(6): p. 867-79.
 21. Fuxe, K., et al., *Volume transmission and its different forms in the central nervous system.* *Chin J Integr Med*, 2013. **19**(5): p. 323-9.
 22. Meguro, Y., et al., *Neuropeptide oxytocin enhances mu opioid receptor signaling as a positive allosteric modulator.* *J Pharmacol Sci*, 2018. **137**(1): p. 67-75.
 23. Heinricher, M.M., S. McGaraughty, and D.A. Farr, *The role of excitatory amino acid transmission within the rostral ventromedial medulla in the antinociceptive actions of systemically administered morphine.* *Pain*, 1999. **81**(1-2): p. 57-65.
 24. Pan, Z.Z., J.T. Williams, and P.B. Osborne, *Opioid actions on single nucleus raphe magnus neurons from rat and guinea-pig in vitro.* *J Physiol*, 1990. **427**: p. 519-32.
 25. Basbaum, A.I. and H.L. Fields, *Endogenous pain control systems: brainstem spinal pathways and endorphin circuitry.* *Annu Rev Neurosci*, 1984. **7**: p. 309-38.
 26. Paxinos, G. and C. Watson, *The rat brain in stereotaxic coordinates.* 4th ed. 1998, San Diego: Academic Press.
 27. Chaure, F.J., H.G. Rey, and R. Quian Quiroga, *A novel and fully automatic spike-sorting implementation with variable number of features.* *J Neurophysiol*, 2018. **120**(4): p. 1859-1871.
 28. Stüttgen, M. *MLIB - toolbox for analyzing spike data version 1.7.0.0.* . 2015; Available from: <https://jp.mathworks.com/matlabcentral/fileexchange/37339-mlib-toolbox-for-analyzing-spike-data>.
 29. Mendell, L.M. and P.D. Wall, *Responses of Single Dorsal Cord Cells to Peripheral Cutaneous Unmyelinated Fibres.* *Nature*, 1965. **206**: p. 97-9.
 30. Schouenborg, J., *Functional and topographical properties of field potentials evoked in rat dorsal horn by cutaneous C-fibre stimulation.* *J Physiol*, 1984. **356**: p. 169-92.
 31. Yizhar, O., et al., *Optogenetics in neural systems.* *Neuron*, 2011. **71**(1): p. 9-34.
 32. Luis-Delgado, O.E., et al., *The transcription factor DeltaFosB is recruited by inflammatory pain.* *J Neurochem*, 2006. **98**(5): p. 1423-31.
 33. Hargreaves, K., et al., *A new and sensitive method for measuring thermal nociception in cutaneous hyperalgesia.* *Pain*, 1988. **32**(1): p. 77-88.



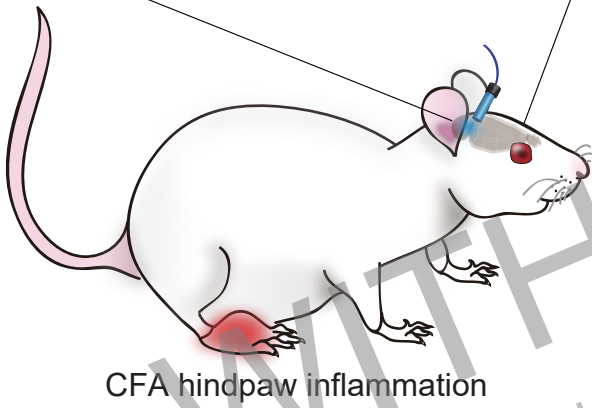
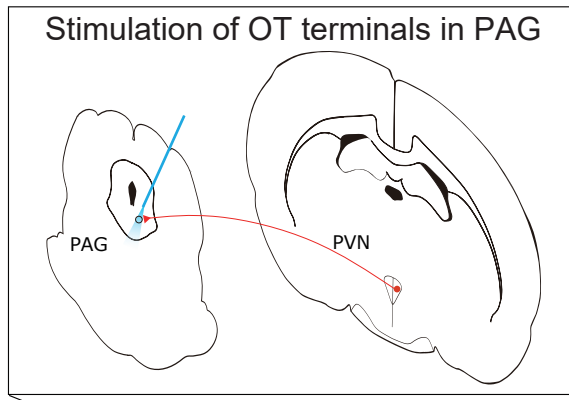
WITHDRAWN
see manuscript DOI for details

Figure 2





A



C

